Computational Materials Science 210 (2022) 111464

Contents lists available at ScienceDirect

Computational Materials Science

journal homepage: www.elsevier.com/locate/commatsci

Full Length Article

Prediction of amorphous forming ability based on artificial neural network and convolutional neural network

Fei Lu [a], Yongchao Liang [a,*], Xingying Wang [b], Tinghong Gao [a], Qian Chen [a], Yunchun Liu [a], Yu Zhou [a], Yongkai Yuan [a], Yutao Liu [a]

[a] School of Big Data and Information Engineering, Guizhou University, Guiyang 550025, China
[b] College of Mechanical and Vehicle Engineering, Taiyuan University of Technology, Taiyuan 030000, China

ARTICLE INFO

Keywords:
Amorphous forming ability
Amorphous alloy
Artificial neural network
Convolutional neural network

ABSTRACT

Using a trial and error method to measure amorphous forming ability in the experiment is a complex and time-consuming process. Therefore, it is necessary to devise a method that can rapidly and accurately predict the amorphous forming ability. In this study, two models, artificial neural network and convolutional neural network, are proposed for the prediction of amorphous forming ability of various amorphous alloys. The prediction accuracy of the two models reached 0.77623 and 0.71693, respectively, both of which were more than 19% higher than the reported prediction accuracy of the 13 criteria. This result shows that artificial neural network and convolutional neural network models can accurately predict the amorphous forming ability of a variety of amorphous alloys and provide theoretical guidance for the development and preparation of amorphous alloys.

1. Introduction

Metallic glasses have received extensive attention due to their excellent physical and mechanical properties such as high strength, high corrosion resistance, low viscosity coefficient, lack of grain, lack of dislocation and lamination defects [1–3]. However, the amorphous forming ability of most metallic glasses is generally poor compared with many commercial oxide glasses [4], which limiting their large-scale applications. The amorphous forming ability is usually evaluated by the critical cooling rate or the critical diameter. The critical cooling rate is a very suitable physical parameter to measure the amorphous forming ability, but it requires tedious and expensive X-ray diffraction experiments or thermal analysis calculations to obtain [5]. Therefore, a large number of scholars have proposed some simple criteria to estimate the critical diameter of metallic glasses through mathematical expressions composed of some easily obtained characteristic parameters to express its amorphous forming ability [6]. These criteria such as γ parameters [7], χ parameters [8] and undercooled liquid region ΔTx [9], etc., but these criteria are only for special alloy compositions and the prediction accuracy is not high, with limitations. Therefore, there is an urgent need for an alternative method to predict the amorphous forming ability of various amorphous alloys.

In recent years, the successful applications of machine learning in various aspects such as speech recognition [10], text classification [11] and medical research [12] have attracted a lot of attention. At the same time, machine learning has also led to great breakthroughs in the field of materials' research. In the study of amorphous forming ability of metallic glasses, Long et al. [13] predicted the amorphous forming ability of amorphous alloys based on K nearest neighbor, gradient boosted decision trees, random forest and extreme gradient boosting, and the prediction results found that extreme gradient boosting predicted the best performance. Cai et al. [14] predicted the critical cooling rate of the alloy based on radial basis function artificial neural network and obtained a reliable model. Ward et al. [15] predicted the critical diameter and undercooled liquid region for bulk metallic glasses based on machine learning, and several alloys were found to exist with higher performance than the original alloy in the range of undercooled liquid region. Deng et al. [4] added other key features based on random forest algorithm to predict the amorphous forming ability of the alloy and improved the prediction accuracy from 57% to 64%. Zhang et al. [16] predicted the critical diameter of metallic glasses using alloy compositions based on a machine learning algorithm, and the predicted results were in good agreement with the experimental values. These studies have illustrated that machine learning provides new ideas and methods

* Corresponding author.
E-mail address: 20113248@qq.com (Y. Liang).

https://doi.org/10.1016/j.commatsci.2022.111464
Received 15 April 2022; Accepted 21 April 2022
Available online 29 April 2022

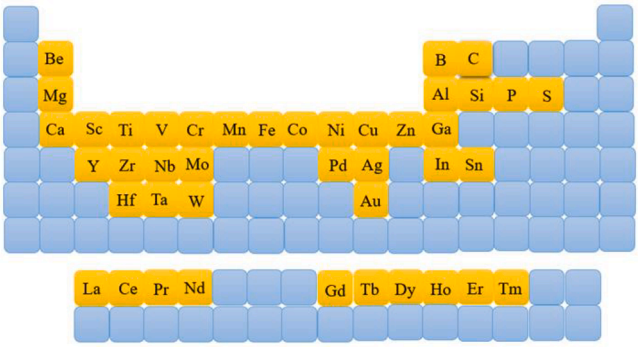

Fig. 1. Elemental distribution of various amorphous alloys in the dataset.

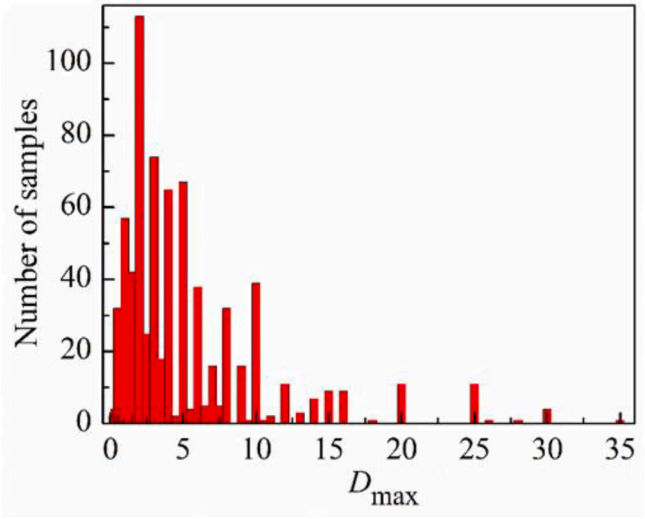

Fig. 2. Overall distribution of critical casting diameters in the dataset.

for exploring the amorphous forming ability of amorphous alloys. Based on this, this paper predicts the critical diameters (D_{max}) of various amorphous alloys corresponding to glass transition temperature (T_g), liquidus temperature (T_l) and onset crystallization temperature (T_x) by artificial neural network (ANN) and convolutional neural network (CNN), and compares the predicted results with the reported 13 criteria.

2. Method

2.1. Data collection

The dataset in this paper is derived from previously published literatures [5], according to which a total of 663 samples containing glass transition temperature, liquidus temperature, onset crystallization temperature and critical diameter were collected. The characteristic temperatures of these samples were obtained by differential thermal analysis and differential scanning calorimetry at a heating rate of 20 K/min, and the critical diameters of the samples were obtained by the copper mold casting method [17]. The dataset contains 42 elements, as shown in Fig. 1.

Fig. 2 shows the overall distribution of critical diameters for 663 samples in the dataset. It can be seen from the figure that the distribution of critical diameters is extremely unbalanced, with the majority of samples with critical diameters below 10 mm and a few distributed in the range of 10 to 35 mm. Therefore, it is highly challenging to use machine learning to predict critical diameter, mainly because machine learning will use samples with smaller critical diameters for intensively trained, which cannot be adequately trained for larger critical diameters [4], so that it is prone to overfitting or underfitting.

2.2. Machine learning

To research the critical diameter associated with amorphous forming ability, ANN and CNN are used to establish the relationship between glass transition temperature, liquidus temperature, and onset crystallization temperature and critical diameter. The machine learning system is shown in Fig. 3, which consists of four main components: building of the dataset, ANN and CNN learning, model evaluation, and prediction.

2.2.1. Artificial neural network

The ANN consists of three parts: the input layer, the hidden layer and the output layer, and its model structure is shown in Fig. 4. The training of ANN is divided into two main parts: forward propagation of information and backward propagation of error. The forward propagation of information is calculated as follows:

$$M_j = \sum_{i=1}^{n} w_{ij} x_i + b_j \tag{1}$$

$$y_j = f(M_j) \tag{2}$$

where x_i is the inputs, w_{ij} is the weight of connection, b_j is the bias, M_j is the input of the hidden layer neuron, f is the activation function, y_j is the output of the hidden layer neuron. After the forward propagation

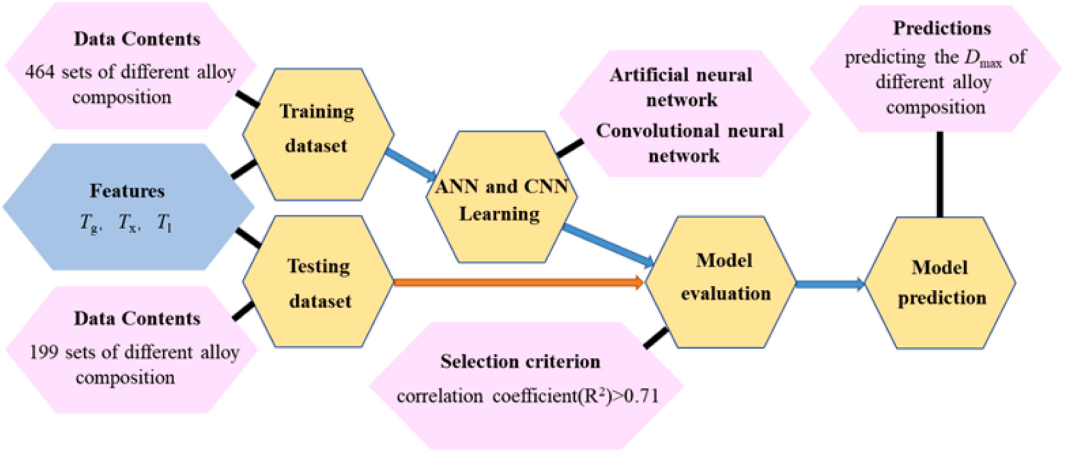

Fig. 3. Flow char of machine learning system.

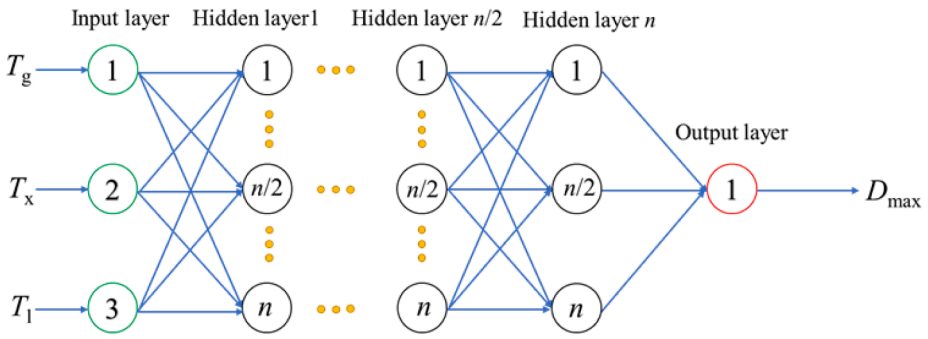

Fig. 4. Structure diagram of artificial neural network model.

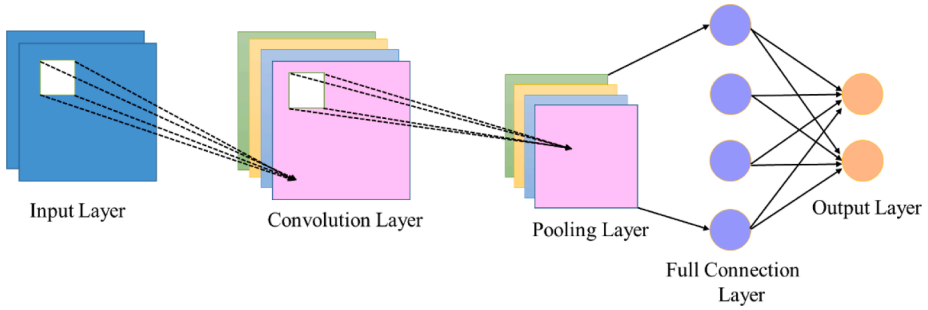

Fig. 5. Structure diagram of convolutional neural network.

process of the information, the global error is calculated, and if the global error is smaller than the desired error, the backward propagation of the error is performed to modify the weights and biases of each layer. The back propagation of the error is calculated as follows:

$$E = \frac{1}{2}\sum_{i=1}^{n}\left(y_i^d - y_i^p\right)^2 \tag{3}$$

$$w_{ij}(k+1) = w_{ij}(k) - \eta\frac{\partial E(k)}{\partial w_{ij}(k)} \tag{4}$$

$$b_{ij}(k+1) = b_{ij}(k) - \eta\frac{\partial E(k)}{\partial b_{ij}(k)} \tag{5}$$

where y_i^d is the desired output of the ANN, y_i^p is the output of the ANN, E is the global error, η is the learning rate, $w_{ij}(k)$ and $b_{ij}(k)$ are the connection weights and biases between layers in the k-th iteration, respectively.

When using ANN to predict the critical diameter, the Relu activation function is used, which has a strong convergence rate and can reduce the training time substantially. The number of hidden layers was determined to be 5 by a trial and error method, where the number of neurons in the five hidden layers were 20, 25, 10, 15 and 20 respectively. In addition, an adam optimizer is used to compile the model, and the learning rate of adam is set to about 0.0012.

2.2.2. *Convolutional neural network*

CNN consists of input layers, convolutional layers, pooling layers, fully connected layers and output layers, of which the convolutional layers and the pooling layers are the most significant parts of the convolutional neural network. The structure of a typical convolutional neural network is illustrated in Fig. 5. The convolutional layer is used to do convolutional operations with the purpose of feature extraction of the input data by convolutional kernels. The pooling layer, also known as the sampling layer, is used to reduce the dimension of the data. The Flatten layer is usually added to CNN, mainly to flatten the data after the pooling layer into a one-dimensional vector [18], so as to facilitate the connection of neurons in the fully connected layer. The process is shown in Fig. 6.

Through continuous attempts, it is determined that the CNN constructed in this paper consists of one input layer, two one-dimensional convolutional layers, one fully connected layer and one output layer.

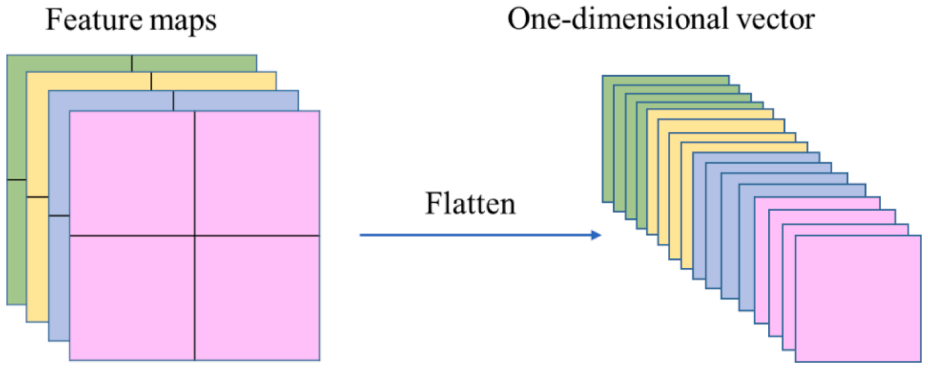

Fig. 6. Flattening process. Four 2*2 feature maps are flattened to a one-dimensional vector with 16 elements.

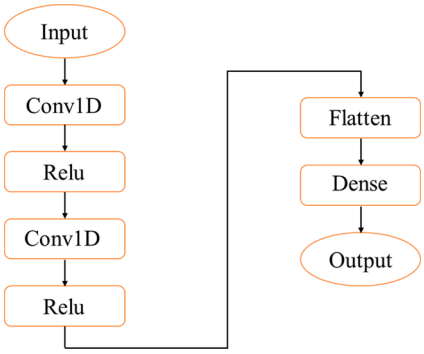

Fig. 7. Structure diagram of One-dimensional convolutional neural network.

Its structure is shown in Fig. 7. The first and second layers of the network are convolutional layers with the number of convolutional kernels of 30 and 10, respectively, the size of the convolutional window is 2, the step size is 1, and Relu is used as the activation function in both layers. The third layer of the network is the Flatten layer. The fourth layer of the network is a fully connected layer with 32 neurons. In addition, the adam optimizer is used to compile the model, and the learning rate of adam is the default value.

2.3. Algorithm model evaluation parameters

To evaluate the performance of ANN and CNN models, we adopt the correlation coefficient (R^2), root mean square error (*RMSE*) and mean absolute error (*MAE*) parameters, whose expressions are as follows:

$$R^2 = \frac{\sum_{i=1}^{N}(x_i-\bar{x})(y_i-\bar{y})}{\sqrt{\sum_{i=1}^{N}(x_i-\bar{x})^2}\cdot\sqrt{\sum_{i=1}^{N}(y_i-\bar{y})^2}} \tag{6}$$

$$RMSE = \sqrt{\frac{1}{N}\sum_{i=1}^{N}(y_i-\bar{y})^2} \tag{7}$$

$$MAE = \frac{1}{N}\sum_{i=1}^{N}|y_i-\bar{y_i}| \tag{8}$$

where y_i is the prediction, $\bar{x}$ is the average of x_i. The larger R^2 and the smaller *RMSE* and *MAE*, the better the predictive performance of the model.

3. Results and discussions

Figs. 8-9 shows the comparison of training and testing results of ANN and CNN models. In these four graphs, the red line indicates the fitted curve between the predicted and measured values, and the black line represents that in the ideal case the predicted value is equal to the measured value. When the red line moves closer to the black line, it indicates the better prediction performance of the model. In Fig. 8**(b)-9 (b)**, it can be seen that some blue points are far away from the black line, indicating that the prediction performance of the model for these samples is not good. The main reason is that the number of these samples is small, resulting in models cannot fully learned.

In order to more intuitively show the prediction effect based on the

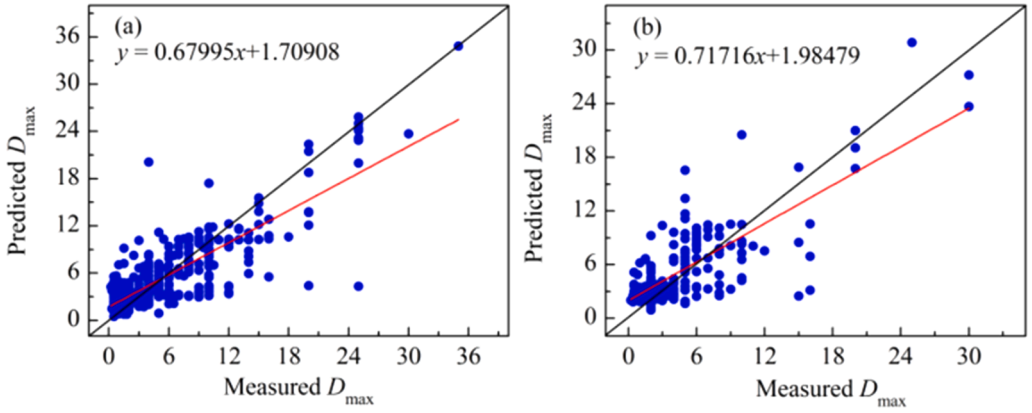

Fig. 8. Comparison between predicted and measured critical diameters by artificial neural network: (a) Training, (b) Test.

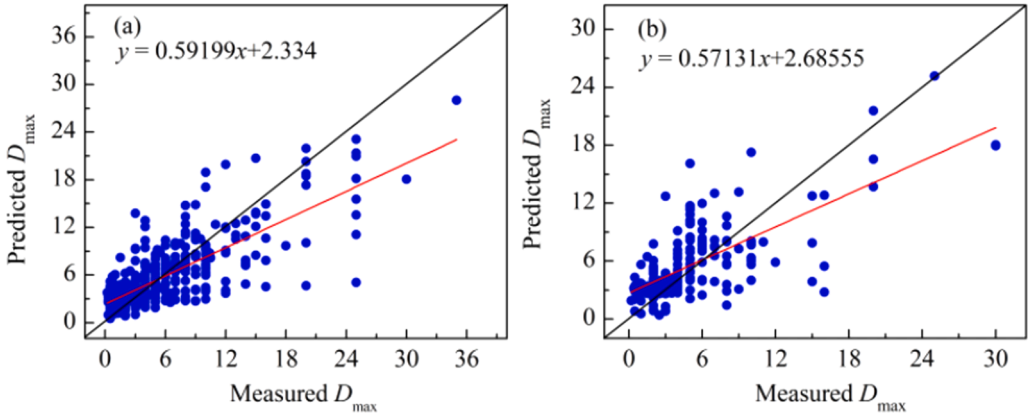

Fig. 9. Comparison between the predicted and measured critical diameters by convolutional neural network: (a) Training, (b) Test.

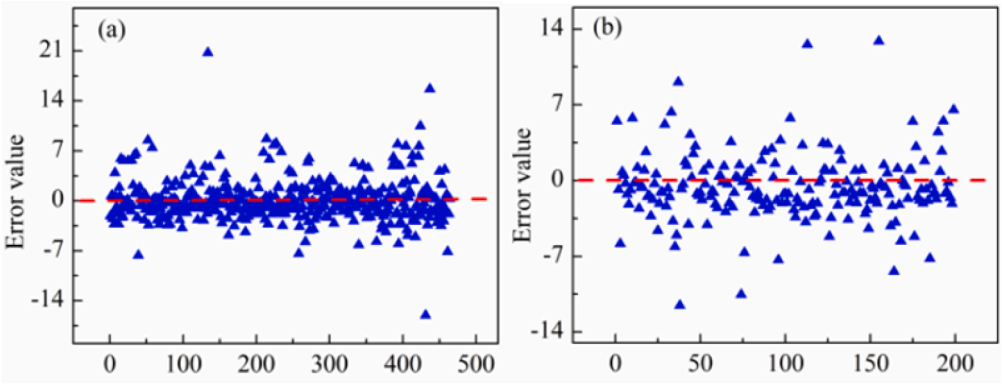

Fig. 10. Scatter plot of prediction error value of artificial neural network: (a) Training, (b) Test.

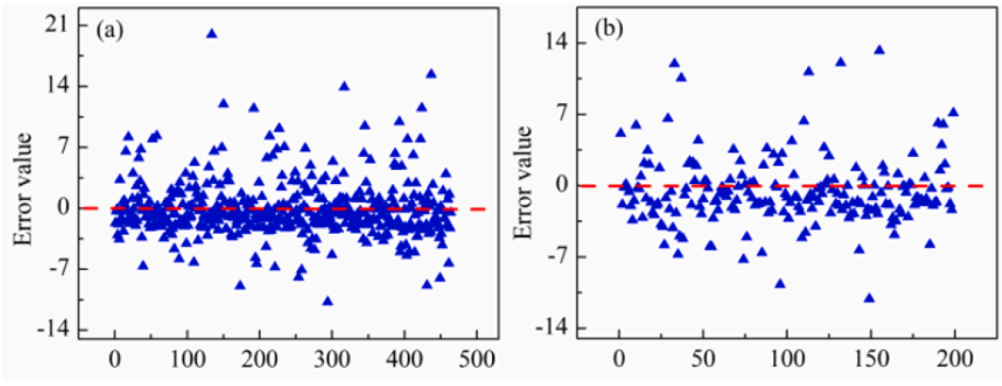

Fig. 11. Scatter plot of prediction error value of convolutional neural network: (a) Training, (b) Test.

Table 1
Evaluation metrics for artificial neural network and convolutional neural network models.

	R^2 train	RMSE train	MAE train	R^2 test	RMSE test	MAE test
ANN	0.82602	2.92367	1.93986	0.77623	3.17085	2.27248
CNN	0.77750	3.26817	2.23667	0.71693	3.42674	2.45520

ANN and CNN models, we make a scatter plot of the error value between the measured value and the predicted value, as shown in Figs. 10-11. The blue triangles in these four plots represent the error value points, and when the error value points are close to 0, it indicates the better prediction performance of the model.

In order to compare the prediction performance of the ANN and CNN models constructed in this paper, we add some criteria for evaluating the amorphous forming ability, and the results are shown in Table 1 and 2. The evaluation results of the ANN and CNN models are given in Table 1. In Table 1 it is shown that the correlation coefficient, root mean square error and mean absolute error of the ANN and CNN models are 0.77623 and 0.71693, 3.17085 and 3.42674, 2.27248 and 2.45520, respectively. The results clearly show that the prediction accuracy of ANN is higher than that of CNN, indicating that the prediction performance of ANN is better than that of CNN. The 13 amorphous forming ability assessment criteria used in this paper and their calculation formulas are given in Table 2. As can be seen in Table 2, the highest prediction accuracy obtained using the amorphous forming ability assessment criterion is 0.60217, both of which are smaller than the prediction accuracy of the ANN and CNN models. ANN improved the prediction accuracy by 29% and CNN improved the prediction accuracy by 19%. The main reason for this improvement is that ANN and CNN have extremely strong data feature extraction capabilities. This result shows that both models can successfully establish the relationship between glass transition temperature, liquidus temperature and onset crystallization temperature and critical diameter, which provides a more reliable basis for determining the amorphous forming ability of amorphous alloys.

In addition, to further improve the prediction accuracy, we use

Table 2
The 13 amorphous forming ability criteria used in this paper and their mathematical formulas.

NO	Criteria	Formula	R^2	References
1	T_{rg}	$T_{rg} = T_g/T_l$	0.24168	[19]
2	δ	$\delta = T_x/(T_l - T_g)$	0.34368	[20]
3	β_r	$\beta_r = (T_x \cdot T_g)/(T_l - T_x)^2$	0.45692	[21]
4	w	$w = T_l \cdot (T_l + T_x)/[T_x \cdot (T_l - T_x)]$	0.48693	[22]
5	ΔT_x	$\Delta T_x = T_x - T_g$	0.44805	[9]
6	γ	$\gamma = T_x/(T_g + T_l)$	0.50375	[7]
7	β_1	$\beta_1 = T_x/T_g + T_g/T_l$	0.51967	[23]
8	γ_m	$\gamma_m = (2T_x - T_g)/T_l$	0.52861	[24]
9	ν	$\nu = T_x \cdot T_g \cdot (T_x - T_g)/(T_l - T_x)^3$	0.59435	[5]
10	w_B	$w_B = (2T_x - T_g)/(T_l + T_x)$	0.53842	[25]
11	γ_c	$\gamma_c = (3T_x - 2T_g)/T_l$	0.55126	[26]
12	χ	$\chi = [(T_x - T_g)/(T_l - T_x)] \cdot [T_x/(T_l - T_x)]^{1.47}$	0.60217	[8]
13	G_p	$G_p = T_g \cdot (T_x - T_g)/(T_l - T_x)^2$	0.5999	[27]

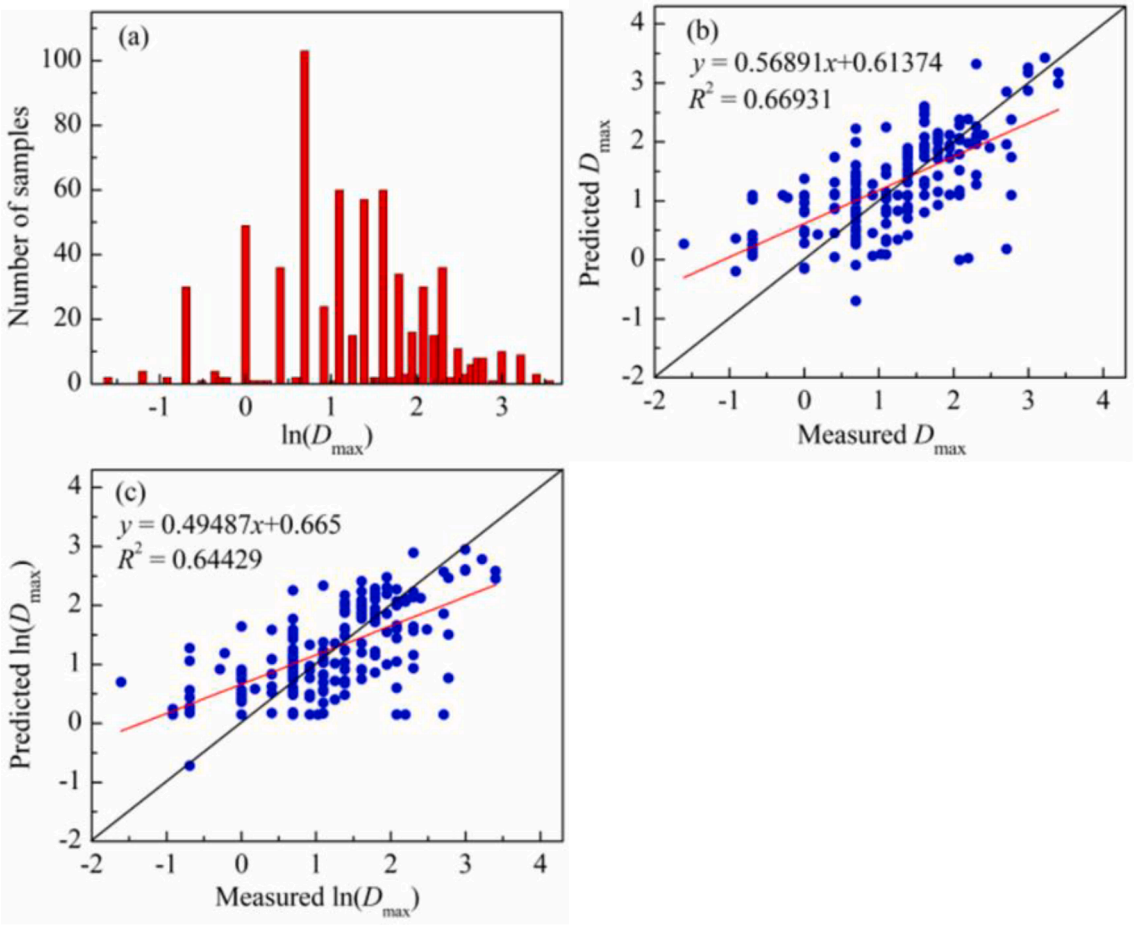

Fig. 12. (a) Distribution of the critical casting diameter after taking the natural logarithm, (b) Comparison between predicted and measured critical diameters by artificial neural network, (c) Comparison between the predicted and measured critical diameters by convolutional neural network.

Deng's method by taking the natural logarithm of the critical diameter, the reason is that the high imbalance of the original critical diameter distribution will lead to difficulty in model training, as shown in Fig. 2. After taking the natural logarithm of the critical diameter, data distribution exhibits stability, which is beneficial to the training of the model, as shown in Fig. 12**(a)**. Surprisingly, after this operation, the ANN and CNN models did not improve the prediction accuracy but decreased it. The prediction accuracy of the ANN and CNN models are reduced to 0.66931 and 0.64429, respectively, as shown in Fig. 12**(b)-(c)**. After transforming the critical diameter by natural logarithm, the prediction accuracy of ANN and CNN did not meet our expectations, the reason may be that the current dataset has a super-imbalanced nature, which makes the model unable to improve the prediction performance [4]. Therefore, we need more sample data, especially for amorphous alloys with relatively large critical diameters, in order to obtain better prediction results.

4. Conclusion

In conclusion, we use machine learning approach to predict the amorphous forming ability of a variety of amorphous alloys, which is based on artificial neural network and convolutional neural network models. Both models can predict the amorphous forming ability of various amorphous alloys, and their prediction accuracy are 0.77623 and 0.71693, respectively, which more than 19% higher than the prediction accuracy of the 13 reported criteria. The main reason for the improved prediction accuracy is that artificial neural networks and convolutional neural networks have extremely strong data feature extraction capabilities. This result shows that both models can successfully establish the relationship between glass transition temperature, liquidus temperature and onset crystallization temperature and critical diameter, which can provide theoretical guidance for the development and preparation of amorphous alloys.

Declaration of Competing Interest

The authors declare that they have no known competing financial interests or personal relationships that could have appeared to influence the work reported in this paper.

Acknowledgements

This work has been supported by the National Natural Science Foundation of China (Grant No. 11964005, 11963003, 62163006, 12004053 and 11764005), The Fostering Project of Guizhou University (Grant No. [2020]33 and [2020]76), Industry and Education Combination Innovation Platform of Intelligent Manufacturing and Graduate Joint Training Base at Guizhou University (Grant No. 2020-520000-83-01-324061).

References

[1] J. Wegner, M. Frey, M. Piechotta, N. Neuber, B. Adam, S. Platt, L. Ruschel, N. Schnell, S.S. Riegler, H.-R. Jiang, G. Witt, R. Busch, S. Kleszczynski, Influence of powder characteristics on the structural and the mechanical properties of additively manufactured Zr-based bulk metallic glass, Mater. Des. 209 (2021) 109976, https://doi.org/10.1016/j.matdes.2021.109976.

[2] J. Li, C. Li, S. Wang, H. Wang, S. Kou, Thermal processing map and thermoplastic forming map of Zr-based bulk metallic glass in the supercooled liquid region, J. Non-Cryst. Solids 570 (2021) 121008, https://doi.org/10.1016/j.jnoncrysol.2021.121008.
[3] W. Guo, M. Wang, Z. Qin, X.u. Shen, S. Lü, X. Chen, S. Wu, Improving the glass-forming ability and plasticity of a TiCu-based bulk metallic glass composite by minor Ta doping, J. Alloy. Compd. 884 (2021) 161054, https://doi.org/10.1016/j.jallcom.2021.161054.
[4] B. Deng, Y. Zhang, Critical feature space for predicting the glass forming ability of metallic alloys revealed by machine learning, Chem. Phys. 538 (2020) 110898, https://doi.org/10.1016/j.chemphys.2020.110898.
[5] R. Deng, Z. Long, L.i. Peng, D. Kuang, B. Ren, A new mathematical expression for the relation between characteristic temperature and glass-forming ability of metallic glasses, J. Non-Cryst. Solids 533 (2020) 119829, https://doi.org/10.1016/j.jnoncrysol.2019.119829.
[6] B. Ren, Z. Long, R. Deng, A new criterion for predicting the glass-forming ability of alloys based on machine learning, Comput. Mater. Sci. 189 (2021) 110259, https://doi.org/10.1016/j.commatsci.2020.110259.
[7] Z.P. Lu, C.T. Liu, A new glass-forming ability criterion for bulk metallic glasses, Acta Mater. 50 (13) (2002) 3501–3512, https://doi.org/10.1016/S1359-6454(02)00166-0.
[8] Z. Long, W. Liu, M. Zhong, Y. Zhang, M. Zhao, G. Liao, Z. Chen, A new correlation between the characteristics temperature and glass-forming ability for bulk metallic glasses, J. Therm. Anal. Calorim. 132 (3) (2018) 1645–1660, https://doi.org/10.1007/s10973-018-7050-0.
[9] A. Inoue, Stabilization of metallic supercooled liquid and bulk amorphous alloys, Acta Mater. 48 (1) (2000) 279–306, https://doi.org/10.1016/S1359-6454(99)00300-6.
[10] L. Deng, G. Hinton, B. Kingsbury, et al., New types of deep neural network learning for speech recognition and related applications: an overview, 2013 IEEE International Conference on Acoustics, Speech and Signal Processing (2013) 8599–8603, https://doi.org/10.1109/ICASSP.2013.6639344.
[11] X. Luo, Efficient English text classification using selected Machine Learning Techniques, Alexandria Eng. J. 60 (3) (2021) 3401–3409, https://doi.org/10.1016/j.aej.2021.02.009.
[12] M.K. Hasan, M.A. Alam, D. Das, E. Hossain, M. Hasan, Diabetes Prediction Using Ensembling of Different Machine Learning Classifiers, IEEE Access 8 (2020) 76516–76531, https://doi.org/10.1109/ACCESS.2020.2989857.
[13] X. Liu, Z. Long, L. Yang, W. Zhang, Z. Li, Prediction of glass forming ability in amorphous alloys based on different machine learning algorithms, J. Non-Cryst. Solids 570 (2021) 121000, https://doi.org/10.1016/j.jnoncrysol.2021.121000.
[14] A.H. Cai, Y. Liu, W.K. An, G.J. Zhou, Y. Luo, T.L. Li, X.S. Li, X.F. Tan, Prediction of critical cooling rate for glass forming alloys by artificial neural network, Mater. Des. (1980-2015) 52 (2013) 671–676, https://doi.org/10.1016/j.matdes.2013.06.012.
[15] L. Ward, S.C. O'Keeffe, J. Stevick, G.R. Jelbert, M. Aykol, C. Wolverton, A machine learning approach for engineering bulk metallic glass alloys, Acta Mater. 159 (2018) 102–111, https://doi.org/10.1016/j.actamat.2018.08.002.
[16] Y.X. Zhang, G.C. Xing, Z.D. Sha, L.H. Poh, A two-step fused machine learning approach for the prediction of glass-forming ability of metallic glasses, J. Alloy. Compd. 875 (2021) 160040, https://doi.org/10.1016/j.jallcom.2021.160040.
[17] L.i. Peng, Z. Long, M. Zhao, Determination of glass forming ability of bulk metallic glasses based on machine learning, Comput. Mater. Sci. 195 (2021) 110480, https://doi.org/10.1016/j.commatsci.2021.110480.
[18] Z. Yang, Y.C. Yabansu, R. Al-Bahrani, W. Liao, A.N. Choudhary, S.R. Kalidindi, A. Agrawal, Deep learning approaches for mining structure-property linkages in high contrast composites from simulation datasets, Comput. Mater. Sci. 151 (2018) 278–287, https://doi.org/10.1016/j.commatsci.2018.05.014.
[19] Z.P. Lu, H. Tan, Y. Li, S.C. Ng, et al., Correlation between reduced glass transition temperature and glass forming ability of bulk metallic glasses, Scr. Mater. 42 (7) (2000) 667–673, https://doi.org/10.1016/S1359-6462(99)00417-0.
[20] Q. Chen, J. Shen, D. Zhang, H. Fan, J. Sun, D.G. McCartney, A new criterion for evaluating the glass-forming ability of bulk metallic glasses, Mater. Sci. Eng., A 433 (1-2) (2006) 155–160, https://doi.org/10.1016/j.msea.2006.06.053.
[21] Z.-Z. Yuan, S.-L. Bao, Y.e. Lu, D.-P. Zhang, L. Yao, A new criterion for evaluating the glass-forming ability of bulk glass forming alloys, J. Alloy. Compd. 459 (1-2) (2008) 251–260, https://doi.org/10.1016/j.jallcom.2007.05.037.
[22] X.-L. Ji, Y.e. Pan, A thermodynamic approach to assess glass-forming ability of bulk metallic glasses, Trans. Nonferrous Metals Soc. China 19 (5) (2009) 1271–1279, https://doi.org/10.1016/S1003-6326(08)60438-0.
[23] K. Mondal, B.S. Murty, On the parameters to assess the glass forming ability of liquids, J. Non-Cryst. Solids 351 (16-17) (2005) 1366–1371, https://doi.org/10.1016/j.jnoncrysol.2005.03.006.
[24] X.H. Du, J.C. Huang, C.T. Liu, Z.P. Lu, New criterion of glass forming ability for bulk metallic glasses, J. Appl. Phys. 101 (8) (2007) 086108, https://doi.org/10.1063/1.2718286.
[25] P. Błyskun, P. Maj, M. Kowalczyk, J. Latuch, T. Kulik, Relation of various GFA indicators to the critical diameter of Zr-based BMGs, J. Alloy. Compd. 625 (2015) 13–17, https://doi.org/10.1016/j.jallcom.2014.11.112.
[26] S. Guo, C.T. Liu, New glass forming ability criterion derived from cooling consideration, Intermetallics 18 (11) (2010) 2065–2068, https://doi.org/10.1016/j.intermet.2010.06.012.
[27] M.K. Tripathi, S. Ganguly, P. Dey, P.P. Chattopadhyay, Evolution of glass forming ability indicator by genetic programming, Comput. Mater. Sci. 118 (2016) 56–65, https://doi.org/10.1016/j.commatsci.2016.02.037.